SYNTHESIS, STRUCTURAL AND OPTICAL CHARACTERIZATION OF GADOLINIUM MIXED YTTRIUM OXIDE NANO MATERIALS

Abstract

Gadolinium mixed Yttrium oxide (Y_2O_3:Gd) nano material shave been synthesized by co-precipitation technique. The synthesized materials have been annealed at 500°C, 750°C and 1000°C using a muffle furnace at normal atmosphere. It is observed that the crystalline nature of the nano powders was increased due to annealing process which is evidenced by the observed diffraction planes in the powder diffraction patterns.In order to identify the oxide vibrations in response to the IR frequency, the FTIR spectra have been recorded and the different modes of vibration of rare earth oxides have been observed. The elemental analysis has been carried out using XPS and energy dispersive spectral analysis using a scanning electron microscope. The weight ratio and atomic ratio of the elements present in the sample has been identified and discussed. The morphology of the annealed samples has been studied through high resolution SEM images and the crystallite size was found by using TEM images. The photo luminescence spectral analysis indicated that the synthesized materials have emission in the blue region. However, it is also observed that the annealing temperature of the samples has influenced significantly on the structure, morphology and photoluminescence property.

Keywords: Rare earth; X-ray diffraction; HRSEM; TEM; PL Spectrum

Authors

P. Anandan
PG & Research Department of Physics
Thiru Kolanjiappar Government Arts College
Vriddhachalam, India
anandantcet@gmail.com

P. Shanmugha Sundaram
PG & Research Department of Physics
Thiru Kolanjiappar Government Arts College
Vriddhachalam, India

T. Saravanan
Centre for Materials Research
Thiruvalluvar College of Engineering and Technology
Vandavasi, India
sarantcet@gmail.com

M. Arivanandhan
Centre for Nanoscience and Technology
Anna University
Chennai, India
arivucz@gmail.com

I. INTRODUCTION

Nanomaterials are being the focused interest of researchers because of their impending applications in various fields of materials science and for the technological development in recent decades. Metal oxides, in particular rare earth oxides and their derivatives have very good electrical, semiconducting and insulating properties which have potential applications in various fields. Especially, rare earth oxides were identified and reported as potential materials for extraordinary luminescent property[1–3]. It has been observed that the doping of other rare earth elements in yttrium oxide has influenced to a greater extent on the enhancement of photoluminescence properties. The emission peak of europium doped yttrium oxide was found to be shifted to the blue region due to the change of crystal field resulting from great surface tension of its nanoscale[4]. Eu doped yttrium oxide nanostructure has been investigated for optical properties with respect to size and it is found that method of preparation has not affected the optical property of Y_2O_3: Eu[5]. However, the incorporation of lithium nano powder in Eu: Y_2O_3prepared by co-precipitation method had enhanced the intensity of luminescence [6].In view of enhancing optical property, europium incorporated Y_2O_3 has been synthesized and reported by several authors[7,8]. Nanocrystalline Y_2O_3/Pr^{3+} have been synthesized by sol-gel process and the photoluminescence property has been reported [9]. Incorporation of Tb^{3+} in yttrium oxide has also been investigated and found that the optical properties have been tuned for the enhancement[10,11]. Recently, Nd^{3+}mixed yttrium oxide has been synthesized and its structural, morphological and photoluminescence property have been reported[12,13]. In recent years, the yttrium oxide nanomaterials are being subjected to analyze the properties of different kind of charged surfactants, as photo active metal oxides, super capacitor applications and in antimicrobial applications[14,15]. Microstructure, cation distribution and magnetic susceptibility with respect to annealing temperature and size of $(Y_{0.9}Gd_{0.1})_2O_3$ have been investigated and reported[16]. Photoluminescence and thermo luminescence properties have been reported for gadolinium doped yttrium oxide phosphor prepared by solid state reaction method[17]. Gama ray induced thermo luminescence studies have been reported in gadolinium doped yttrium oxide prepared by solid state reaction[18]. Along with structural and morphological investigation, thermo luminescence glow curve has been obtained for gadolinium doped yttrium oxide nanophosphor and the parameters such as activation energy and trap depth, order of kinetics and frequency have been obtained [19].

However, limited works have been reported on gadolinium mixed yttrium oxide nanomaterials on their structural and photoluminescence characteristics. Hence, it is aimed to prepare the gadolinium mixed yttrium oxide nonmaterial and to study its structural, morphological and photoluminescence properties. Various nanostructures of rare earth yttrium oxides with different morphologies have been synthesized by methods like sol-gel [9,20], thermal decomposition [21], solvo-thermal [22] co-precipitation [23], auto-ignition [24], etc., and their properties were investigated. Among these methods, co-precipitation method has been widely used as it is simple and effective method for the preparation of rare earth oxides[23]. Hence, in this work, Y_2O_3:Gd has been prepared by co precipitation technique. The Y_2O_3:Gd has been prepared by replacing yttrium precursor with ten molar weight percent of gadolinium precursor. The synthesized materials were subjected to structural, morphological and photoluminescence characterization and discussed in this chapter.

II. SYNTHESIS

Bulk nano particles of gadoliniummixed Y_2O_3 have been synthesized by co-precipitation method. In a typical synthesis of gadolinium mixed Y_2O_3 nanomaterials, aqueous yttrium nitrate hexahydrate solution was prepared by dissolving yttrium nitrate hexahydrate (0.09 M) in Millipore water (resistance ~18MΩ) with ten weight percentage (0.01M) of Gadolinium trichloride hexahydrate. This aqueous solution was stirred well and the required amount of ammonia solution was added drop wise. After constant stirring at room temperature for 3 h, the white precipitate was collected and dried overnight at 70°C to remove the solvent. The dried particles were washed with ethanol and water several times in order to remove the ionic impurities. The possible chemical reaction for the formation of Y_2O_3:Gdnanomaterials can be expressed as,

$$(0.09M)Y(NO_3)_3\,6H_2O + (0.01M)Gd(Cl)_3\,6H_2O \rightarrow Y^{3+} + Gd^{3+} + 3Cl_3^- + 6H_2O \quad (1)$$

$$Y^{3+} + Gd^{3+} + 3NH_4OH \rightarrow Y(1-x)Gdx(OH)_3 + 3NH_4^+ \quad (2)$$

$$2Y(1-x)Gdx(OH)_3 \xrightarrow{O_2} Y_2O_3{:}Gd + 3H_2O \quad (3)$$

$Y(NO_3)_3.6H_2O$ and $GdCl_3.6H_2O$ decomposes to form Y^{3+} and Gd^{3+} along with their byproducts as shown in Equation (1). The OH^- in the base reactant reacts with the acid reactant of Y^{3+} in the solution, resulting in homogeneous precipitation. As per Equation (2) $Y(OH)_3$ is formed through the hydrolysis of Y^{3+} followed by the oxidation of O_2 from air to form Y_2O_3 (Equation (3)). In order to improve the crystalline nature of the as-prepared sample, it was annealed at 500°C, 750°C and 1000°C for 3 h in a muffle furnace.

III. CHARACTERIZATION TECHNIQUES

The XRD analysis was conducted in reflection mode using a X'Pert Pro diffractometer with Cu Kα radiation (λ=1.5406 Å). The scanning rate was set at 1°/min, covering the 2θ range from 20° to 80°. For FTIR spectra, the as-prepared Y_2O_3:Gd nanomaterials annealed at 1000°C were recorded using a NICOLET Infrared spectrophotometer. X-ray photoelectron spectra were obtained using a Shimadsu ESCA 3400 electron spectrophotometer. For surface morphology and elemental analysis, a High-resolution scanning electron microscope (HRSEM) equipped with an energy dispersive analyzer of X-rays (EDAX) system was utilized. Transmission electron microscope (TEM) images and selected-area electron diffraction (SAED) patterns were obtained using a JEOL JEM-200 CX model at 200 kV. To study the photoluminescence, a Jobin Yvon Fluorolog-3-TAU steady-state/lifetime spectro fluoro meter was employed, covering the wavelength range of 200–900 nm for both the as-prepared samples and those annealed at 500°C, 750°C, and 1000°C..

IV. RESULTS AND DISCUSSION

1. **Powder XRD Analysis:** Powder XRD patterns of Gadolinium mixed Y_2O_3 as-prepared nanomaterials and annealed at 750°C and 1000°C temperatures are compared in Figure 1. The XRD patterns of as-prepared samples show amorphous nature with some humps around 30° and 45°, which is the indication of Y_2O_3 compound formation in the mixed Yttrium oxide as well. The amorphous nature observed in the as-prepared sample may be

due to the hydroxide compound of Yttrium. When the samples are annealed at higher temperatures, the hydroxides have been transformed into oxide, which is confirmed by the powder XRD patterns obtained for the annealed samples. The XRD patterns of the annealed (at 750°C and 1000°C) samples, confirm the cubic phase of Y_2O_3nanomaterials (JCPDS #83-0927), with lattice constant a = 10.6108 Å.The calculated lattice constant is reflected in almost all the lattice planes of the XRD patterns of Y_2O_3:Gd nanomaterials with only meager variations. Hence,It is inferred from the XRD patterns of Y_2O_3:Gd nanomaterials that there is no significant variation in the crystal structure due to annealing. However,a meager peak shift towards lower diffraction angle due to annealing at higher temperature has been observed in the pattern as shown in the Figure 1(B) which may due to lattice reorientation during the crystallization process at higher temperature. Also, the annealing at higher temperature has influenced to increase the crystallite size as expected. The dislocation density and stacking fault also have been calculated and found that these values have been decreased as the annealing temperature has been increased as shown in the table 1.

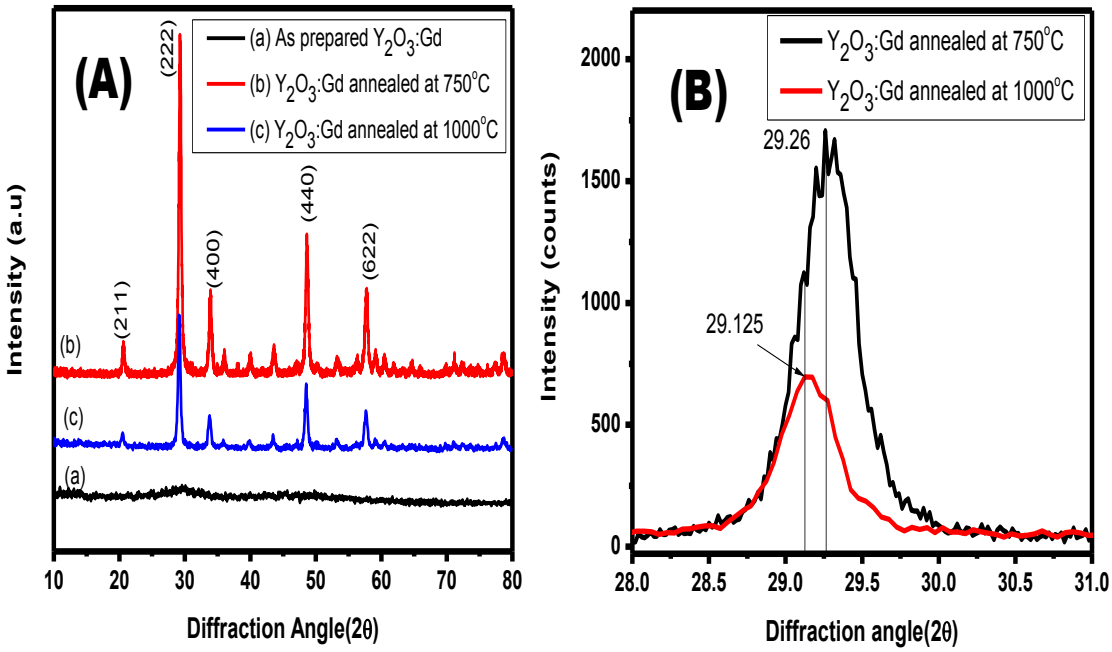

Figure 1: Powder XRD patterns of (A) as-prepared and annealed Y_2O_3:Gdnanomaterialsat 750°C and 1000°C temperatures in air (B) Comparison of the peak for 222 diffraction planes**.**

Table 1: Comparison of Powder diffraction data of Y_2O_3:Gdnano particles annealed at 750°C and 1000°C

hkl	Pos. [°2Th.]		FWHM [°2Th.]		Crystallite Size [nm]		Dislocation Density (x 10^{15} lines/m^2)		Sacking fault (Å)	
	750° C	1000° C	750° C	1000 °C	750° C	1000° C	750° C	1000° C	750°C	1500°C
211	20.62	20.48	0.36	0.41	22.44	19.76	1.986	2.562	0.002523	0.002885
222	29.26	29.13	0.44	0.41	18.67	19.83	2.869	2.542	0.002149	0.002031
400	33.92	33.75	0.48	0.45	17.31	18.45	3.337	2.938	0.002006	0.001892
440	48.62	48.49	0.50	0.44	17.44	19.82	3.287	2.545	0.001411	0.001245
622	57.74	57.60	0.60	0.48	15.12	19.20	4.371	2.764	0.001387	0.001106

2. **FTIR Spectral Analysis:** FTIR spectra of as prepared and annealed samples of Y_2O_3:Gd nano materials were recorded by NICOLET Infrared spectrophotometer as shown in Figure 4.8. FTIR spectra of Y_2O_3:Gd nano materials contains O-H stretching vibration at 3490 cm^{-1}. The weak intense peak around 1650 cm^{-1} is due to hydroxyl group in the water is also absorbed by the sample from the atmosphere. The intense peak around 1530 cm^{-1}, 1400 cm^{-1} and 629 cm^{-1} are due to the stretching vibrations of rare earth element with oxygen. The shift in the peaks due to annealing effect has been observed and tabulated in Table 2.

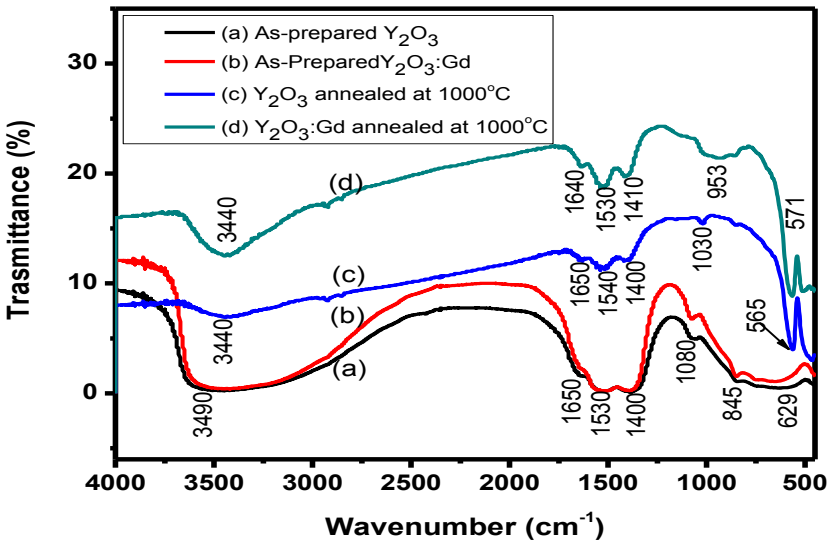

Figure 2: FTIR spectra of as-prepared and annealed samples of Y_2O_3:Gd

Table 2: Wave numbers of important vibrations observed and their assignments

Sl. No.	Wavenumbers				Assignment
	As-Prepared		Annealed at 1000°C		
	Y_2O_3	$Gd:Y_2O_3$	Y_2O_3	$Gd:Y_2O_3$	
1	3490	3490	3440	3440	O-H stretching
2	1530	1530	1540	1530	C-O asymmetric stretching
3	1400	1400	1400	1410	C-O asymmetric stretching
4	1080	1080	1030	953	C-O asymmetric stretching
5	629	629	565	571	Y-O stretching

3. **X-Ray Photoelectron Spectral Analysis:** Figure 3 represents the XPS wide spectra obtained for pure Y_2O_3 and Y_2O_3:Gd nanomaterials annealed at 750°C. The spectra exhibit signals corresponding to Y 3d, C 1s, and O 1s electrons at their respective binding energies. Further analysis is shown in Figure 4, where (a) displays the core level X-ray photoelectron spectra of Y 3d electrons for pure Y_2O_3, and (b) shows the same for Y_2O_3:Gd.

For pure Y_2O_3, the Y 3d core level spectrum displays a single intense signal of electrons with a binding energy of 158.6 eV. This signal reveals two peaks related to Y $3d^{5/2}$ and Y $3d^{3/2}$ electrons, with respective binding energies of 157.8 eV and 159.6 eV, showing a difference of approximately 1.8 eV between them. In the case of Y_2O_3:Gd, the binding energy of the single peak observed remains unchanged. However, on deconvolution, two signals related to Y $3d^{5/2}$ and Y $3d^{3/2}$ electrons are observed, with slightly increased binding energies of 0.4 eV and 0.6 eV, respectively. This finding indicates that the incorporation of doping elements is favorable, as it does not significantly weaken the binding nature of Y 3d electrons.

Similarly, in the core level spectra of 1s electrons for the prominent element Oxygen (O) in both pure Y_2O_3 and Y_2O_3:Gd samples (Figs. 4c&d), the signal appears at a binding energy of 530.6 eV, with the phenomenon of unaltered binding energy due to the dopants being observed. However, on deconvolution, it is noted that the single peak in both cases contains two signals. In pure Y_2O_3, the binding energies of the oxygen signals are measured at 530.4 eV and 532.1 eV, with the former corresponding to lattice oxygen and the latter to oxygen diffused to the surface due to the annealing process. In Y_2O_3:Gd, the binding energy of lattice oxygen shows only a marginal change of 0.1 eV. The consistent binding energies of Y 3d and O 1s electrons in both cases provide evidence that Gd has been successfully incorporated into the lattice structure.

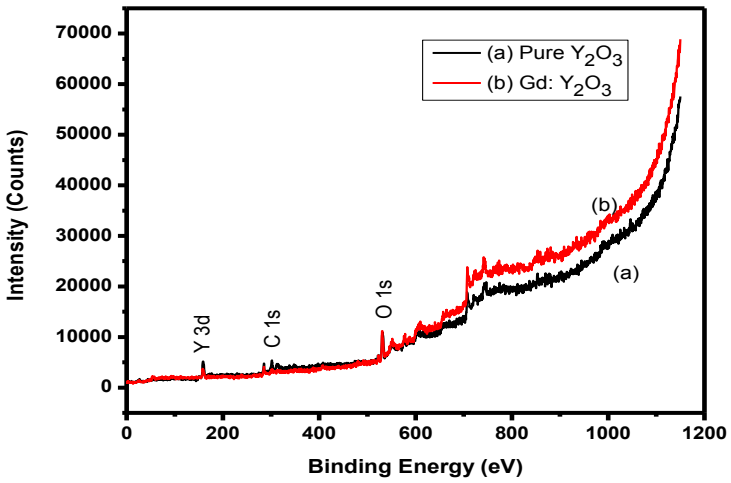

Figure 3: XPS spectra of as-prepared (a) pure Y_2O_3 and (b) Y_2O_3:Gdshows the signal for Y 3d, C1s and O1s electrons

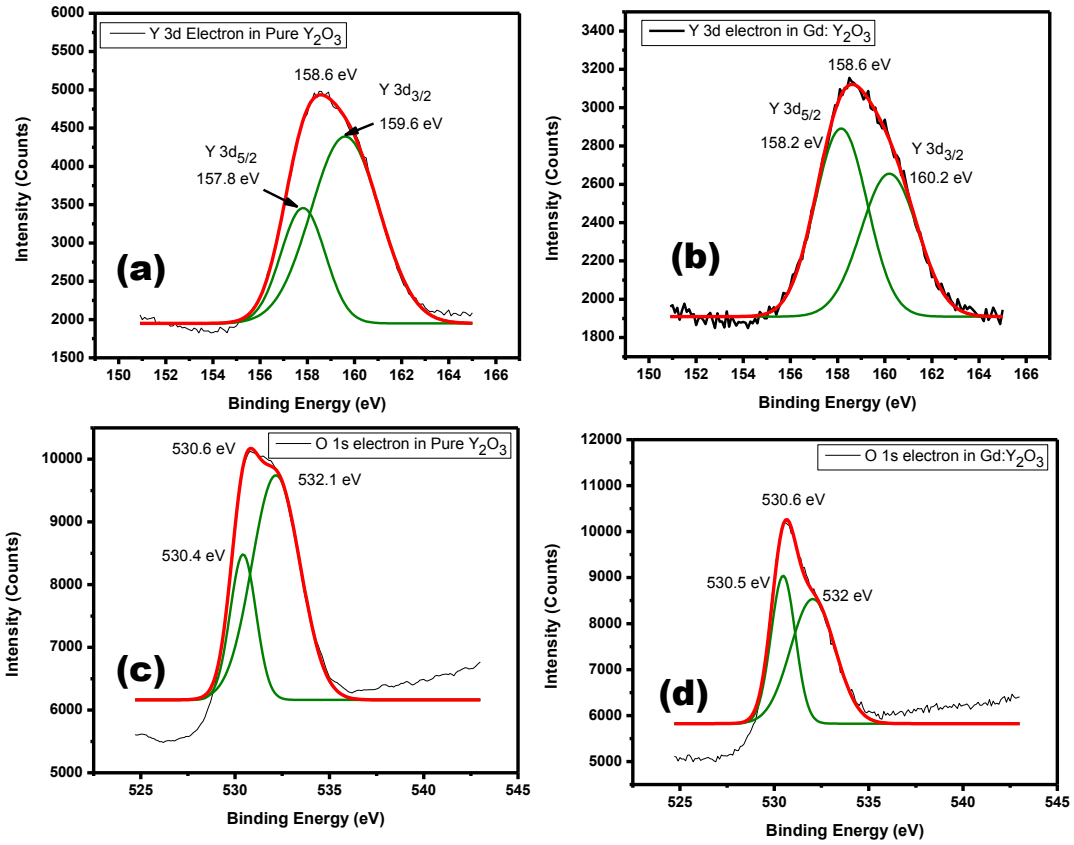

Figure 4: Core level XPS spectra of (a&b) Yttrium 3d electrons from Pure and Y_2O_3:Gd, (c&d) Oxygen1s electron obtained from Pure and Y_2O_3:Gd

Furthermore, the core level spectra of 3d and 4d electrons of the dopant element (gadolinium) present in Y_2O_3:Gd samples are depicted in Figure 5 (a&b). On deconvolution of the Gd 3d electron signal, two distinct peaks related to Gd $3d^{5/2}$ and Gd $3d^{3/2}$ are observed

at 1236.3 eV and 1241.2 eV, respectively. Additionally, the Gd 4d electron signal shows a doublet related to Gd $4d^{5/2}$ and Gd $4d^{3/2}$, observed at 142 eV and 150 eV, respectively, with a nearly 8 eV separation in binding energy. These observed signals of gadolinium's 3d and 4d electrons serve as a signature of its presence in Y_2O_3:Gd.

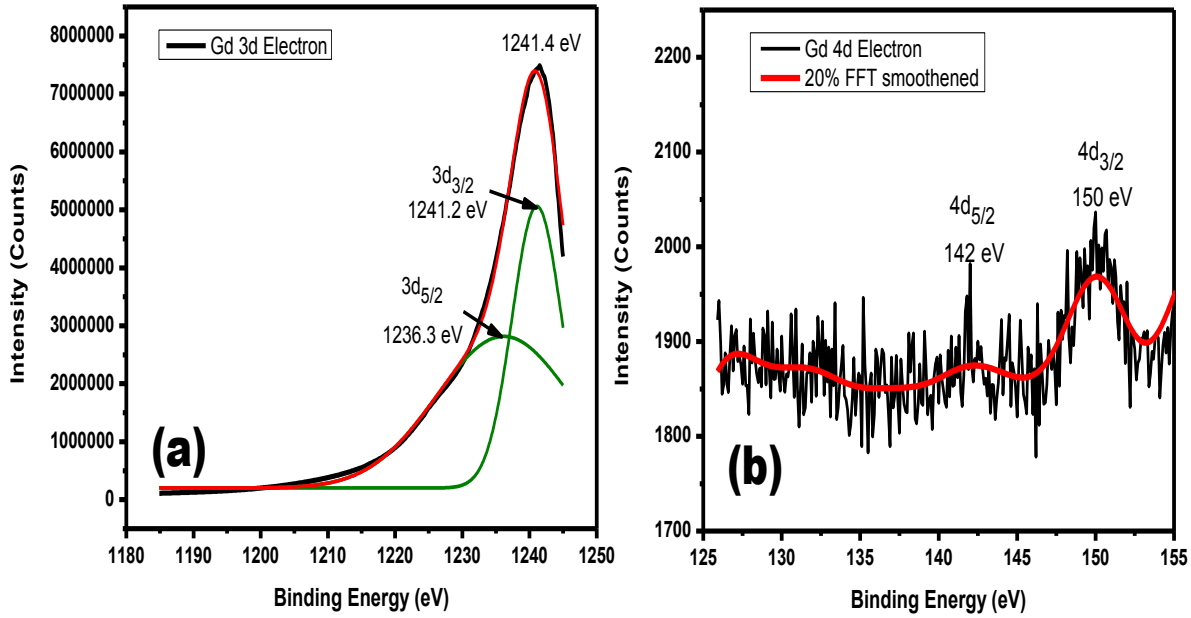

Figure 5: Core level XPS spectra of Gadolinium (a) 3d electron and (b) 4d electron signals obtained from Y_2O_3:Gd

4. **EDS and Morphological Analysis:** The Y_2O_3:Gd nanomaterial was subjected to elemental analysis using a scanning electron microscope equipped with an energy dispersive analyzer of X-rays (EDAX) system. The SEM images, along with the energy dispersive spectrum of Y_2O_3:Gd, are presented in Figure 6(a-c). The elemental compositions of the samples are tabulated in the inset of Figure 6c, revealing that 5.95 weight percentages of gadolinium have been successfully incorporated into the Yttrium oxide nanostructures. Surface morphology was further studied using High-resolution scanning electron microscopy (HRSEM) images. The HRSEM images of as-prepared Gadolinium-mixed Y2O3 nanomaterials, in two different magnifications, are displayed in Figure 6(a&b). From the images, it is evident that the mixed samples exhibit irregular shapes with no significant difference. However, the crystalline nature of the Gadolinium-mixed samples is high, indicating the agglomeration/aggregation of the powder samples to form a highly crystalline structure.

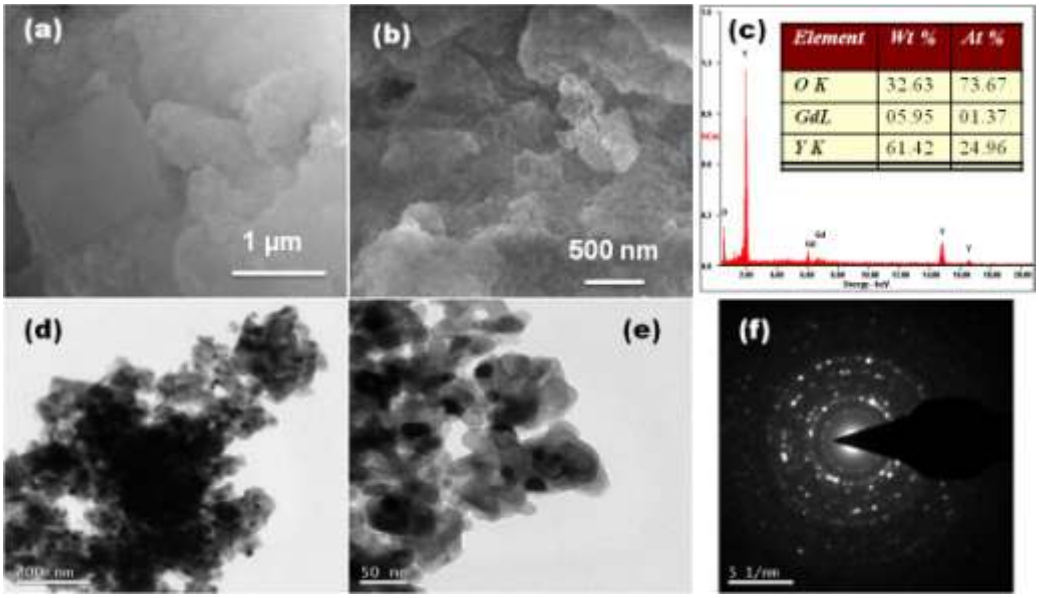

Figure 6: HRSEM images and Energy dispersive spectrum (a-c) and TEM images of Y_2O_3:Gdsample annealed at 750°C at different magnification along with SAED Pattern(d-f). The inset of 'c' shows the elemental composition**.**

Transmission electron microscopy (TEM) images of Y_2O_3:Gd samples at both low and high magnifications are shown in Figure 6(d&e). The TEM images confirm that the particle sizes are less than 50 nm. Additionally, the selected area electron diffraction (SAED) pattern demonstrates that the particles possess high crystalline order, as evidenced by the presence of bright dots in the rings, as shown in Figure 6f.

5. **Photoluminescence Spectral Analysis:** Photoluminescence (PL) analysis was conducted using a JobinYvon Fluorolog-3-TAU steady-state/lifetime spectrofluorometer in the wavelength range of 200–900 nm. Figure 7 illustrates the PL spectra of both pure Y_2O_3 nanomaterials and Gadolinium-mixed Y_2O_3 nanomaterials when excited at a wavelength of 350 nm.

In the PL spectra of Gadolinium-mixed Y_2O_3 nanomaterials, a distinct violet/blue light emission peak is observed at 434 nm. This emission peak can be attributed to the charge transfer from the 4f band to the valence band of Y_2O_3, as reported in previous studies [25]. Upon annealing the samples, the emission peak remains nearly at the same wavelength as that of the as-prepared sample; however, there is a significant variation in the intensity. Additionally, new peaks at 532 nm and 572 nm are observed with increased intensity. These observations suggest that the host emission at 434 nm has been suppressed, and the defect level emission at 532 nm and 572 nm has been enhanced due to the annealing process. The change in emission characteristics after annealing indicates alterations in the luminescence behavior, likely influenced by the structural and compositional modifications during the thermal treatment.

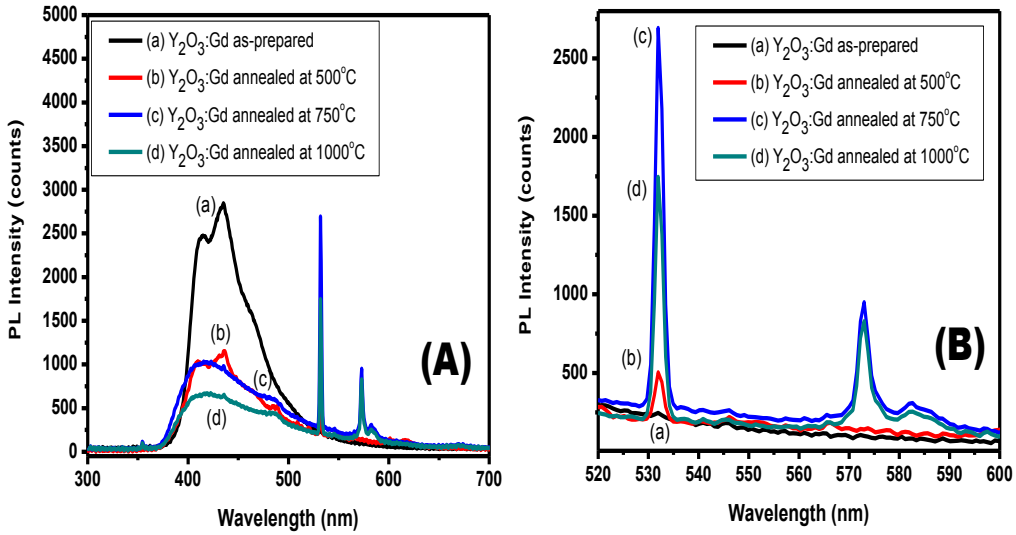

Figure 7: PL spectra of Y_2O_3: Gdfor 350 nm light excitation in the region between (A) 300-700 and (B) 520 - 600.

V. CONCLUSION

In conclusion, a comprehensive characterization of Gadolinium-mixed Y_2O_3 nanomaterials was performed through various analytical techniques, including XRD, FTIR, XPS, EDS, morphology, and photoluminescence analyses. X-ray diffraction (XRD) analysis revealed that the as-prepared samples exhibited an amorphous nature, with indications of Y_2O_3 compound formation in the mixed Yttrium oxide. Upon annealing at higher temperatures, the hydroxide compounds transformed into oxides, confirmed by the presence of the cubic phase of Y_2O_3 nanomaterials. FTIR spectra showed distinctive peaks representing O-H stretching vibrations at 3490 cm^{-1}, as well as weak intense peaks related to hydroxyl groups absorbed from the atmosphere. Additionally, intense peaks at 1530 cm^{-1}, 1400 cm^{-1}, and 629 cm^{-1} were observed, corresponding to the stretching vibrations of rare earth elements with oxygen. The shift in these peaks due to annealing effects was also observed. X-ray photoelectron spectra (XPS) provided insights into the binding energies of Y 3d and O 1s electrons, indicating the successful incorporation of gadolinium into the lattice structure without significantly weakening the binding nature of Y 3d electrons. Energy-dispersive X-ray spectroscopy (EDS) analysis further confirmed the presence and elemental compositions of the samples. Surface morphology was studied through high-resolution scanning electron microscopy (HRSEM), which revealed the irregular shape of the mixed samples, with enhanced crystallinity and increased crystallite size upon annealing at higher temperatures. Photoluminescence (PL) analysis showcased a violet/blue light emission peak at 434 nm for Gadolinium-mixed Y_2O_3 nanomaterials, attributed to the charge transfer from the 4f band to the valence band of Y_2O_3. Annealing at higher temperatures resulted in suppressed host emission at 434 nm, with an increase in defect level emission at 532 nm and 572 nm.

Overall, the combined results from XRD, FTIR, XPS, EDS, morphology, and photoluminescence analyses provide a comprehensive understanding of the structural,

compositional, and luminescent properties of Gadolinium-mixed Y_2O_3nanomaterials. These findings are crucial for exploring the potential applications of these nanomaterials in various technological domains.

REFERENCES

[1] Bazzi R, Flores-Gonzalez MA, Louis C, Lebbou K, Dujardin C, Brenier A, et al. Synthesis and luminescent properties of sub-5-nm lanthanide oxides nanoparticles. Journal of Luminescence 2003;102–103:445–50. https://doi.org/10.1016/S0022-2313(02)00588-4.

[2] Cho I, Kang J-G, Sohn Y. Photoluminescence profile imaging of Eu(III), Tb(III) and Eu(III)/Tb(III)-doped yttrium oxide nanosheets and nanorods. Journal of Luminescence 2015;157:264–74. https://doi.org/10.1016/j.jlumin.2014.09.006.

[3] Zhang X, Wang Y, Cheng F, Zheng Z, Du Y. Ultrathin lanthanide oxides nanomaterials: synthesis, properties and applications. Sci Bull 2016;61:1422–34. https://doi.org/10.1007/s11434-016-1155-2.

[4] Yongqing Z, Zihua Y, Shiwen D, Mande Q, Jian Z. Synthesis and characterization of Y2O3:Eu nanopowder via EDTA complexing sol–gel process. Materials Letters 2003;57:2901–6. https://doi.org/10.1016/S0167-577X(02)01394-0.

[5] Zhang W-W, Zhang W-P, Xie P-B, Yin M, Chen H-T, Jing L, et al. Optical properties of nanocrystalline Y2O3:Eu depending on its odd structure. Journal of Colloid and Interface Science 2003;262:588–93. https://doi.org/10.1016/S0021-9797(03)00169-3.

[6] Hou X, Zhou S, Li Y, Li W. Luminescent properties of nano-sized Y2O3:Eu fabricated by co-precipitation method. Journal of Alloys and Compounds 2010;494:382–5. https://doi.org/10.1016/j.jallcom.2010.01.054.

[7] Pandey A, Pandey A, Roy MK, Verma HC. Sol–gel synthesis and characterization of Eu+++/Y2O3 nanophosphors by an alkoxide precursor. Materials Chemistry and Physics 2006;96:466–70. https://doi.org/10.1016/j.matchemphys.2005.07.037.

[8] Wu X, Tao Y, Gao F, Dong L, Hu Z. Preparation and photoluminescence of yttrium hydroxide and yttrium oxide doped with europium nanowires. Journal of Crystal Growth 2005;277:643–9. https://doi.org/10.1016/j.jcrysgro.2005.01.098.

[9] Daniele S, Hubert-Pfalzgraf LG. Synthesis of nanocrystalline Y2O3/Pr3+ from heterometallic alkoxide via sol–gel process. Materials Letters 2004;58:1989–92. https://doi.org/10.1016/j.matlet.2003.12.021.

[10] Muenchausen RE, Jacobsohn LG, Bennett BL, McKigney EA, Smith JF, Valdez JA, et al. Effects of Tb doping on the photoluminescence of Y2O3:Tb nanophosphors. Journal of Luminescence 2007;126:838–42. https://doi.org/10.1016/j.jlumin.2006.12.004.

[11] Serantoni M, Mercadelli E, Costa AL, Blosi M, Esposito L, Sanson A. Microwave-assisted polyol synthesis of sub-micrometer Y2O3 and Yb-Y2O3 particles for laser source application. Ceramics International 2010;36:103–6. https://doi.org/10.1016/j.ceramint.2009.07.002.

[12] Kolesnikov IE, Mamonova DV, Lähderanta E, Kolesnikov EY, Kurochkin AV, Mikhailov MD. Synthesis and characterization of Y2O3:Nd3+ nanocrystalline powders and ceramics. Optical Materials 2018;75:680–5. https://doi.org/10.1016/j.optmat.2017.11.032.

[13] Anandan P, Sankar R, Selvakumar V, Saravanan T, Arivanandhan M, Hayakawa Y, et al. Effect of Neodymium substitution on the structural, morphological and optical properties of yttrium oxide nanocrystals. Materials Research Innovations 2022;0:1–10. https://doi.org/10.1080/14328917.2022.2085005.

[14] Morsi RE, El-Salamony RA. Effect of cationic, anionic and non-ionic polymeric surfactants on the stability, photo-catalytic and antimicrobial activities of yttrium oxide nanofluids. Journal of Molecular Liquids 2020;297:111848. https://doi.org/10.1016/j.molliq.2019.111848.

[15] Saravanan T, Raj SG, Chandar NRK, Jayavel R. Synthesis, Optical and Electrochemical Properties of Y2O3 Nanoparticles Prepared by Co-Precipitation Method. Journal of Nanoscience and Nanotechnology 2015;15:4353–7. https://doi.org/10.1166/jnn.2015.9802.

[16] Kremenovic A, Antic B, Nikolic AS, Blanusa J, Jancar B, Meden A, et al. The dependence of cation distribution, microstrain and magnetic susceptibility on particle size in nanocrystalline Gd2O3/Y2O3. Scripta Materialia 2007;57:1061–4. https://doi.org/10.1016/j.scriptamat.2007.09.002.

[17] Dubey V, Agrawal S, Kaur J. Photoluminescence and thermoluminescence behavior of Gd doped Y2O3 phosphor. Optik 2015;126:1–5. https://doi.org/10.1016/j.ijleo.2014.06.175.

[18] Tamrakar RK, Upadhyay K, Bisen DP. Gamma ray induced thermoluminescence studies of yttrium (III) oxide nanopowders doped with gadolinium. Journal of Radiation Research and Applied Sciences 2014;7:526–31. https://doi.org/10.1016/j.jrras.2014.08.012.
[19] Tamrakar RK, Dubey V. Synthesis, structural characterization and thermoluminescence glow curve study of gadolinium-doped Y2O3 nanophosphor. Journal of Taibah University for Science 2016;10:317–23. https://doi.org/10.1016/j.jtusci.2014.11.002.
[20] Kuang Q, Lin Z-W, Lian W, Jiang Z-Y, Xie Z-X, Huang R-B, et al. Syntheses of rare-earth metal oxide nanotubes by the sol–gel method assisted with porous anodic aluminum oxide templates. Journal of Solid State Chemistry 2007;180:1236–42. https://doi.org/10.1016/j.jssc.2007.01.021.
[21] Pižl M, Jankovský O, Ulbrich P, Szabó N, Hoskovcová I, Sedmidubský D, et al. Facile preparation of nanosized yttrium oxide by the thermal decomposition of amorphous Schiff base yttrium complex precursor. Journal of Organometallic Chemistry 2017;830:146–9. https://doi.org/10.1016/j.jorganchem.2016.12.018.
[22] Huang G, Zhanglian H, Shizhu Z, Pengyue Z, Xianping F. Synthesis of Yttrium Oxide Nanocrystal via Solvothermal Process. Journal of Rare Earths 2006;24:47–50. https://doi.org/10.1016/S1002-0721(07)60319-6.
[23] Srinivasan R, Yogamalar R, Bose AC. Structural and optical studies of yttrium oxide nanoparticles synthesized by co-precipitation method. Materials Research Bulletin 2010;45:1165–70. https://doi.org/10.1016/j.materresbull.2010.05.020.
[24] Hari Krishna R, Nagabhushana BM, Nagabhushana H, Chakradhar RPS, Sivaramakrishna R, Shivakumara C, et al. Auto-ignition based synthesis of Y2O3 for photo- and thermo-luminescent applications. Journal of Alloys and Compounds 2014;585:129–37. https://doi.org/10.1016/j.jallcom.2013.09.037.
[25] Krishna Chandar N, Jayavel R. Synthesis and photoluminescence properties of HMT passivated Dy2O3 nanoparticles. Physica E: Low-Dimensional Systems and Nanostructures 2012;44:1315–9. https://doi.org/10.1016/j.physe.2012.02.010.

